Partial decortication ameliorates dopamine depletion-induced striatal neuron lesions in rats

YAOFENG ZHU[1,2*], BINGBING LIU[3*], XUEFENG ZHENG[1], JIAJIA WU[4], SI CHEN[5], ZHI CHEN[1], TAO CHEN[1], ZIYUN HUANG[1] and WANLONG LEI[1]

[1]Department of Anatomy, Zhongshan School of Medicine, Sun Yat-sen University, Guangzhou, Guangdong 510080; [2]Institute of Medicine, College of Medicine, Jishou University, Jishou, Hunan 416000; [3]Department of Anesthesiology, Guangdong Second Provincial General Hospital, Guangzhou, Guangdong 510317; [4]Periodical Center, The Third Affiliated Hospital, Sun Yat-sen University, Guangzhou, Guangdong 510630; [5]Institute of Biomedical and Pharmaceutical Sciences, Guangdong University of Technology, Guangzhou, Guangdong 510006, P.R. China

Received March 3, 2019; Accepted June 27, 2019

DOI: 10.3892/ijmm.2019.4288

Abstract. The balance between glutamate (cortex and thalamus) and dopamine (substantia nigra) inputs on striatal neurons is of vital importance. Dopamine deficiency, which breaks this balance and leads to the domination of cortical glutamatergic inputs, plays an important role in Parkinson's disease (PD). However, the exact impact on striatal neurons has not been fully clarified. Thus, the present study aimed to characterize the influence of corticostriatal glutamatergic inputs on striatal neurons after decortication due to dopamine depletion in rats. 6-Hydroxydopamine was injected into the right medial forebrain bundle to induce dopamine depletion, and/or ibotenic acid into the primary motor cortex to induce decortication. Subsequently, the grip strength test and Morris water maze task indicated that decortication significantly shortened the hang time and the latency that had been increased in the rats subjected to dopamine depletion. Golgi staining and electron microscopy analysis showed that the total dendritic length and dendritic spine density of the striatal neurons were decreased in the dopamine-depleted rats, whereas decortication alleviated this damage. Immunohistochemistry analysis demonstrated that decortication decreased the number of caspase-3-positive neurons in the dopamine-depleted rats. Moreover, reverse transcription-quantitative PCR and western blot analyses showed that decortication offset the upregulation of caspase-3 at both the protein and mRNA levels in the dopamine-depleted rats. In conclusion, the present study demonstrated that a relative excess of cortical glutamate inputs had a substantial impact on the pathological processes of striatal neuron lesions in PD.

Correspondence to: Dr Wanlong Lei, Department of Anatomy, Zhongshan School of Medicine, Sun Yat-sen University, 74 Zhongshan Road 2, Guangzhou, Guangdong 510080, P.R. China
E-mail: leiwl@mail.sysu.edu.cn

*Contributed equally

Key words: dopamine depletion, striatal lesion, decortication, Parkinson's disease, rat

Introduction

Striatal dopamine insufficiency is a major contributor to the motor symptoms of PD (1,2). The striatum, which is the main component of the basal ganglia, is a mass-like structure formed by a cluster of cells. In rodents, 90-95% of striatal neurons are projection neurons, which are involved in performing striatal functions and are simultaneously regulated by striatal interneurons (3). Importantly, striatal projection neurons receive both excitatory inputs from the cerebral cortex and thalamus and inhibitory inputs from the substantia nigra pars compacta (SNc). Then, the striatal neurons provide feedback to the striatum and cerebral cortex after relaying through the substantia nigra and thalamus, which exert regulatory functions on the striatum (4-7). Neurotransmitter inputs target striatal neurons (especially projection neurons), and coordination of the excitatory and inhibitory inputs maintains the structural integrity and functional stability of the striatal neurons (8). Striatal dopamine depletion leads to an imbalance among the cortex, thalamus and SNc; thus, dopamine depletion induces a relative increase in corticostriatal glutamatergic inputs, which is considered the main mechanism underlying striatal neuronal damage (9,10). If the excitatory input to the cortical striatum is reduced after striatal dopamine deprivation, the balance between excitability and inhibitory input on striatal neurons can be restored. A partial decortication approach was used in the present study to decrease corticostriatal glutamatergic inputs(Fig. S1).

The pathological mechanisms underlying striatal neuron injury after dopamine depletion induced by 6-hydroxydopamine (6OHDA) remain unclear. When the dopaminergic input from the midbrain is removed, a result is a relative increase in cortical excitatory input to the striatal neurons, which is also considered a possible cause. The loss of dopaminergic neurons in the substantia nigra results in striatal dopamine neurotransmitter depletion. Striatal dopamine depletion induces an

imbalance between excitatory and inhibitory afferents to the striatum and leads to morphological changes and complex physiological changes in the striatum (11,12). A previous study confirmed that 6OHDA-induced PD rats exhibited behavioral disorders associated with striatal function, such as muscular tension, learning, memory and cognitive deficits (13). The present study examined the effect of decortication on dopamine depletion-induced behavioral disorders. Changes have also previously been identified in the morphology and protein and gene expression levels of striatal neurons in PD rat models (14,15). One study showed that the neuronal damage manifests as the loss of dendritic spines (16). Although other reports have described apoptotic changes in striatal neurons (17-19), the potential mechanisms remain unclear. To determine whether the changes in striatal neurons were associated with the relative increase in glutamatergic inputs, dopamine depletion, glutamate depletion and dopamine + glutamate depletion models were used to investigate histopathological and protein changes in striatal neurons (Fig. S1).

In light of the aforementioned findings, the present study aimed to confirm the lesion mechanism of striatal neurons and the regulatory effects of cortical glutamatergic inputs in PD pathological processes, which is of importance for further understanding of the pathological mechanisms of PD.

Materials and methods

Experimental animals. Male 8-week-old Sprague-Dawley (SD) rats weighing 200-250 g were used for the present study. All rats were obtained from the Center for Experimental Animals of Sun Yat-sen University. All rat care and procedures involved were approved by the Animal Care and Use Committee of Sun Yat-sen University (no. SYXK GUANGDONG 2011-0029). Animal welfare and experimental procedures were carried out strictly in accordance with the Guide for the Care and Use of Laboratory Animals (Guide for Ethical Review of Animal Welfare of China, 2018) (20). The SD rats were individually housed in an air-conditioned room (temperature 22±0.5˚C, relative humidity, 40-70%) under a 12 h light-dark cycle, with water and food available *ad libitum*.

SD rats (n=96) were randomly assigned to the control group (n=24), 6OHDA group (n=24), ibotenic acid (IA) group (n=24) and 6OHDA+IA group (n=24). In each group, six animals were used for Golgi-Cox staining, six for immunohistochemistry and electron microscopy (EM) detection, and six for western blotting; the remaining animals were used for reverse transcription-quantitative (RT-q)PCR.

For clarity and conciseness, the data and statistical analyses presented in the text include only the control, 6OHDA, IA and 6OHDA+IA groups unless otherwise indicated.

Treatment of animals. 6OHDA is a neurotransmitter analog that is used to induce nigrostriatal dopamine depletion (21). IA is a neurotoxic isoxazole that is used to induce corticostriatal glutamate depletion. The rats were deeply anesthetized with sodium pentobarbital [50 mg/kg, intraperitoneal (i.p.); cat. no. P3761; Sigma-Aldrich; Merck KGaA] and fixed on a Kopf stereotaxic frame (Stoelting Co.). Burr holes were made in the skull over the primary motor cortex (M1) and the right medial forebrain bundle (MFB). The rats in the 6OHDA group were injected with 8 μl 6OHDA (2 μg/μl; 6OHDA dissolved in 0.9% saline containing 0.01% ascorbic acid as an antioxidant; cat. no. H116; Sigma-Aldrich; Merck KGaA) in the right MFB [anterior-posterior (AP), -3.6; medial-lateral (ML), -0.19; and dorsal ventral (DV), -8.2] using a 10 μl syringe (Hamilton Company). The PD rat models used in the present study were described in a previous report (22). The rats in the IA group were injected with 1 μl of 45 nM IA (CAS no. 2552-55-8; Sigma-Aldrich; Merck KGaA) in the primary motor cortex (AP, -1.7; ML, -2.2; and DV, -1.7). The rats in the 6OHDA+IA group were injected with both 6OHDA and IA on the right side using the same methods (16,23). The rats in the vehicle control group were injected with solvent at the same volume in the same injection location. The rats in the 6OHDA vehicle control group were injected with 8 μl solvent (0.9% saline containing 0.01% ascorbic acid) in the right MFB. The rats in the IA vehicle control group were injected with 1 μl solvent (0.9% saline) in the primary motor cortex. The rats in the 6OHDA+IA vehicle control group were injected with both 6OHDA solvent and IA solvent on the right side using the same methods.

During the 3 weeks following 6OHDA lesions, rats were subcutaneously injected with apomorphine (APO; cat. no. 2073/50; Tocris Bioscience) at a dose of 0.25 mg/kg, and the number of 360˚ contralateral rotations within 30 min were counted. Only rats with a significant number of contralateral rotations (>7 cycles/minute or >210 total cycles) were included. The effect of APO on motor asymmetry and rotation to the uninjured side (the left in the present study) in a 30 min period were recorded by two examiners who were blinded to animal states. The rotation behavior test method was described in detail in a previous study (14). All rats were sacrificed at 28 days after surgery and further examined. All brains were quickly removed and used for Golgi-Cox staining, immunohistochemistry, EM detection, western blotting and RT-qPCR. Moreover, immunohistochemical staining for tyrosine hydroxylase was performed to ensure the success of the model after slicing. Only the data and tissue from the rats with TH-positive fibers (<5%) in the right striatum were used in the subsequent analyses. The extent of TH-positive fibers after 6OHDA lesion development was shown in a previous study (13). The APO-induced rotation test and immunohistochemical staining of TH were designed to ensure that successful dopamine depletion-induced PD models were used for further examination (data not shown) and have been described previously (13,14). A total of 4 weeks after development of the IA lesions, the focal cortical lesions were examined using a light microscope (LM).

Behavioral tests

Grip strength test. During the 3 weeks following the 6OHDA lesions, the grip strength of each rat was evaluated by recording the time spent hanging on a steel wire that was 2 mm in diameter and 35 mm in length, and suspended 50 cm above the horizontal surface of the ground (24). The test was performed three times/day over a 5 day period. All animals underwent these test (n=24/group). The observers were blinded to the rat treatment conditions.

Morris water maze task. During the 3 weeks following the 6OHDA lesions, the rats were trained twice a day for 5 days. All animals underwent these tests (n=24/group). A probe test was

conducted on the last day of the Morris water maze task (25). During the training process, the target platform (diameter, 10 cm) was located in a fixed position. In each session, the animals were released from four designated starting points (north, east, south and west) and allowed to swim until they reached the target platform or for 2 min. Once the rats reached the platform or failed to find the platform within 2 min, they remained on the platform for 30 sec. In each session, the latency to reach the platform within 2 min was recorded using the TopScan™ 2.0 behavior analysis system (CleverSys, Inc.).

Golgi staining. The methods for Golgi staining were previously described in detail (26). At 4 weeks following the 6OHDA lesions, all the rats were deeply anesthetized with sodium pentobarbital (50 mg/kg, i.p.) and perfused with 0.9% saline. The brains were harvested and stained using the FD Rapid GolgiStain™ kit in accordance with the manufacturer's instructions (cat. no. PK 401; FD Neuro Technologies.). The brains were first stored in the dark for 14 days in Golgi-Cox solution and then submerged in 30% sucrose for 3 days. The brains were sectioned coronally at a thickness of 50 μm using a vibratome (Leica VT1200S; Leica Microsystems GmbH). Sections were collected and the stain was developed with ammonium hydroxide for 30 min. Sections were immersed in deionized water for another 30 min and then washed with water, dehydrated, cleared and mounted using a resin. Dendrites and dendritic spines were photographed using a Leica DM 2500B microscope equipped with a x40 objective. The Neuron J v1.4.1 software (National Institutes of Health) was used to measure the total dendrite lengths and spine numbers. The dendrite and dendritic spine morphologies were examined in the striatal neurons and the data were analyzed using Sholl analysis (27). The third dendrite order of the striatal neurons from the dorsal-lateral striatum of each group was quantitatively analyzed with regard to the spine numbers. In the present study, the experimental area of interest was the dorsal-lateral zone of the striatum, which is the sensorimotor area of the striatum. The location of this region in the striatum was described in an earlier study (15). The dendritic spine densities were measured on dendritic segments 10 μm in length. The densities of dendritic spine were determined on striatal neurons from the dorsal-lateral striatum. In Golgi-stained slices, the total dendritic length was calculated by summing the lengths of each branch segment within a dendrite and then summing the total lengths of each of the dendrites for each neuron. The spine numbers from 10 μm of the dendrite were counted as spine density (28).

Immunohistochemistry. During the 4 weeks following 6OHDA lesions, rats (n=3/group) were anesthetized with 0.4% pentobarbital sodium at 50 mg/kg and perfused transcardially with PBS (500 ml; 0.1 M) followed by 500 ml of 4% paraformaldehyde (in 0.1 M phosphate buffer, pH 7.4). The brain tissue samples were then removed and immersed in 4% paraformaldehyde overnight at 4˚C. The brain tissue was cut into 30 μm sections with a vibratome. The sections were pretreated with 0.3% H_2O_2 and 0.1% Triton-X 100 for 30 min at room temperature. BSA (3%; Sigma-Aldrich; Merck KGaA; cat. no. B2064) was used to block non-specific binding sites at room temperature for 30 min. The sections were incubated at 4˚C for 24 h with the following primary antibodies: Mouse anti-TH (1:1,000; EMD Millipore; cat. no. MAB318) diluted with 0.1 M PBS (pH 7.4) containing 0.5% BSA and 0.3% Triton X-100. The sections were rinsed and incubated in anti-mouse IgG (1:200; Sigma-Aldrich; Merck KGaA; cat. no. M4280) diluted with the aforementioned buffer for 3 h at room temperature, followed by incubation in homologous PAP complex (1:200; Sigma-Aldrich; Merck KGaA; cat. no. P1291) at room temperature for 2 h. The peroxidase reaction was performed using 3,3'-diaminobenzidine (0.05% in 0.1 M PBS, pH 7.4; Sigma-Aldrich; Merck KGaA; cat. no. 11718096001) at room temperature for 1-2 min. Sections were mounted onto gelatin-coated slides, dehydrated, permeabilized with xylene and covered with neutral balsam.

To perform conventional double-label immunofluorescence, sections were incubated overnight at 4˚C with primary antibody. The primary antibodies were mouse anti-NeuN (1:800; EMD Millipore; cat. no. 2884594) and rabbit anti-caspase-3 (1:500; Cell Signaling Technology, Inc.; cat. no. 9662) diluted with 0.1 M PBS, pH 7.4, containing 0.5% BSA and 0.3% Triton X-100. The sections were subsequently incubated with anti-mouse fluorescent IgG (1:200; Alexa Fluor 480; Molecular Probes; cat. no. A11029; Thermo Fisher Scientific, Inc.) and anti-rabbit fluorescent IgG (1:200; Alexa Fluor 594; Molecular Probes; Thermo Fisher Scientific, Inc.; cat. no. A32740) for 3 h at room temperature. The section containing the striatum was observed by confocal microscopy (Nikon C2; Nikon Corporation; magnification x20). The number of positive cells was counted in five randomly selected squares (100x100 μm) in the dorsal-lateral striatum.

EM. During the 4 weeks following the 6OHDA lesions, rats (n=3/group) used for EM were perfused in the aforementioned manner (as per the immunohistochemistry analysis), but 0.6% glutaraldehyde was added to the fixative. All brains were quickly removed and immersed in 4% paraformaldehyde + 15% saturated picric acid in 0.1 M PB overnight at 4˚C, then sectioned at 50 μm by vibratome. Five sections were used in the EM analysis for each animal. The methods of EM used were previously described in detail (26). The processed slices were rinsed in sodium cacodylate buffer (0.1 M, pH 7.2), then postfixed with 2% osmium tetroxide (cat. no. 18456; PELCO; Ted Pella, Inc.) for 1 h, dehydrated in a graded series of ethyl alcohols, impregnated with 1% uranyl acetate in 100% alcohol, and flat-embedded in Spurr's resin (cat. no. 18010; PELCO Eponate 12™ kit; Ted Pella, Inc.). All sections were examined with an LM. The dorsal-lateral striatal areas were cut from the slide and glued to the top of a resin block. The slices were mounted on mesh grids and stained with 0.4% lead citrate and 4.0% uranyl acetate using an LKB ultramicrotome (cat. no. EM UC6; Leica Microsystems, GmbH). The EM Tecnai G2 Spirit Twin (FEI; Thermo Fisher Scientific, Inc.) was used to examine the tissue sections. The number of dendritic spines was counted in the area of the dorsal-lateral striatum using the captured images. For the EM data, the analysis and quantification were carried out on digital EM images. Five nonoverlapping squares with a size of 100 μm^2 in each image were selected. The number of spines/100 μm^2 was counted as the spine density. For each animal, the analysis was based on 30 EM images (29).

Table I. Measurements from and comparisons between the behavioral tests.

Test items	Group			
	Control	6OHDA	IA	6OHDA+IA
Hang time, sec	11.67±2.16	22.17±1.47[a]	14.67±2.66[a,b]	12.83±1.72[b]
Latency, sec	40.0±16.91	92.56±17.18[a]	42.61±32.09	45.50±17.86[b]

Values are expressed as the group mean ± SD; one-way ANOVA followed by least significant difference post hoc tests. [a]P<0.05 vs. control; [b]P<0.05 vs. 6OHDA group. 6OHDA, 6-hydroxydopamine; IA, ibotenic acid.

Western blotting. During the 4 weeks following the 6OHDA lesions, rats (n=6/group) were sacrificed by decapitation after deep anesthesia with sodium pentobarbital (50 mg/kg, i.p.), and the striatum of each rat was extracted and homogenized. The striatal tissue was extracted and lysed with RIPA buffer (Beyotime Institute of Biotechnology). Protein was quantified using a bicinchoninic acid kit (Beyotime Institute of Biotechnology). A total of 30 μg protein sample was separated by SDS-PAGE (10%) and transferred onto a PVDF membrane (cat. no. IPVH00010; EMD Millipore). After the transfer, the membranes were blocked with 5% dried skim milk in Tris-buffered saline with Tween-20 at room temperature for 1.5 h and then incubated and shaken overnight at 4˚C with the following primary antibodies: Rabbit anti-caspase-3 (1:5,000; Cell Signaling Technology, Inc.; cat. no. 9662), rabbit anti-cleaved caspase-3 (1:2,500; Cell Signaling Technology, Inc.; cat. no. 9661) and rabbit anti-β-actin (1:2,000; EMD Millipore; cat. no. ABT1485). The membranes were incubated with horseradish peroxidase (HRP)-conjugated goat-anti-rabbit IgG antibody (1:5,000; cat. no. AP307P; EMD Millipore) for 2 h at room temperature. The immunoreactive bands were visualized with chemiluminescent HRP substrate (cat. no. WBKLs0500; EMD Millipore). The protein bands were visualized using a Bio-Rad GelDoc XR+ system (Bio-Rad Laboratories, Inc.) and quantified using ImageJ v1.8.0 software (National Institutes of Health).

RT-qPCR. During the 4 weeks following the 6OHDA lesions, rats (n=6/group) were sacrificed by decapitation after deep anesthesia with sodium pentobarbital (50 mg/kg, i.p.), and the striatum of each rat was extracted from the brain. According to the manufacturer's instructions, total RNA was isolated using TRIzol® reagent (Invitrogen; Thermo Fisher Scientific, Inc.). cDNA was synthesized using the SuperScript VILO cDNA Synthesis kit (cat. no. 11754250, Invitrogen; Thermo Fisher Scientific, Inc.). The samples were kept at 42˚C for 60 min on the PCR instrument, after which they were kept at 70˚C for 5 min to inactivate the reverse transcriptase. qPCR was performed with SYBR-Green Master Mix (ABI; Thermo Fisher Scientific, Inc.) on an ABI PRISM 7000 Sequence Detection (Applied Biosystems; Thermo Fisher Scientific, Inc.) under the following conditions: 50˚C for 5 min, 95˚C for 10 min, followed by 45 cycles at 95˚C for 30 sec and 60˚C for 30 sec. Relative gene expression was analyzed using the $2^{-\Delta\Delta Cq}$ method (30). The primers were as follows: Caspase-3 forward, 5'-GGACCTGTGGACCTGAAAAA-3'; Caspase-3 reverse, 5'-GCATGCCATATCATCGTCAG-3'; β-actin forward, 5'-GAACCCTAAGGCCAAC-3'; and β-actin reverse, 5'-TGTCACGCACGATTTCC-3'. The cycling conditions were previously described (22). The melting curves were analyzed using the 7500 system SDS software v.2.0.6 (Applied Biosystems™; Thermo Fisher Scientific, Inc.; cat. no. 4377354).

Statistical analysis. The investigators were blinded when analyzing the morphological data. IBM SPSS Statistics v22.0 software (IBM Corp.) was used for all statistical analyses. Data are expressed as the mean ± SD. Least significant difference post hoc tests were used to examine the statistical significance among the four groups. Behavioral indicators were examined by one-way ANOVA followed by least significant difference post hoc tests. Comparisons among groups were examined by two-way analysis of variance, and P<0.05 was considered to indicate a statistically significant difference.

Results

Decortication alleviates the behavioral dysfunction induced by dopamine depletion in the PD rat model. As reported in a previous study, muscular tension is markedly upregulated in rats treated with 6OHDA to eliminate dopaminergic neurons (13). The grip strength test showed that the hanging time was significantly increased in the 6OHDA group (22.17±1.47 sec) compared with the control group (11.67±2.16 sec) and the IA group (14.67±2.66 sec; P<0.05). Notably, the hanging time was significantly decreased in the 6OHDA+IA group (12.83±1.72 sec; P<0.05; Table I) compared to the 6OHDA group, and slightly decreased compared to the IA group.

Cognitive deficits are common clinical symptoms of PD that seriously affect the quality of life of patients. Thus, the water maze task was used to investigate the cognitive deficits in the experimental rat model. The probe trial of the Morris water maze task showed that the latency of the 6OHDA group (92.56±17.18 sec) was significantly longer than that of the control group (40.0±16.91 sec; P<0.05), whereas the latency of the 6OHDA+IA group (45.50±17.86 sec) was significantly shorter than that of the 6OHDA group (92.56±17.18 sec; P<0.05; Table I).

Motor dysfunction caused by upregulated muscle tension, and cognitive deficits, are the main clinical symptoms of PD. These results indicated that decortication alleviated the behavioral dysfunction induced by dopamine depletion in the PD rat model.

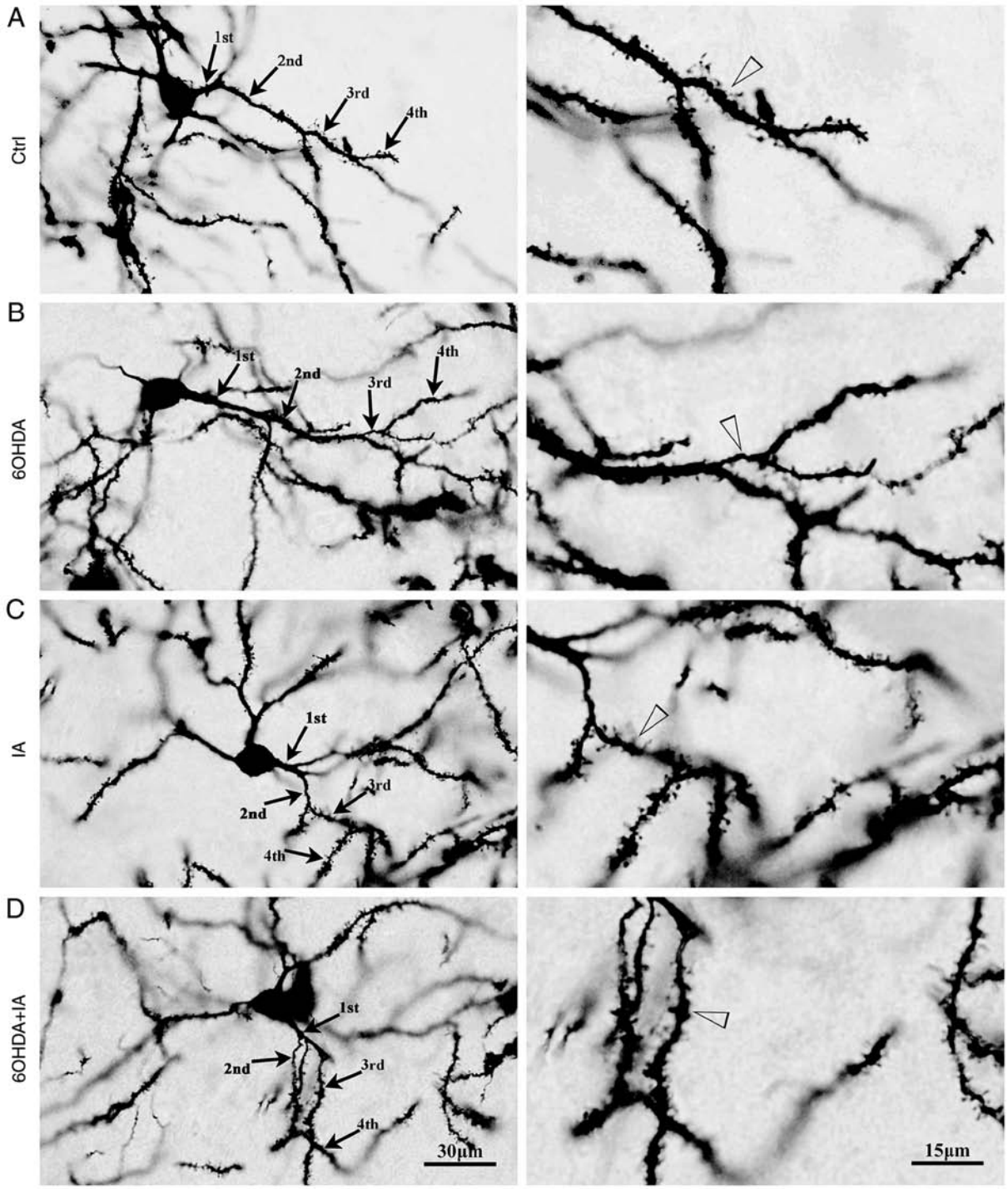

Figure 1. Detection of dendrites and dendritic spines on striatal neurons via Golgi staining. (A) Images from rats in the control group; (B) images from rats in the 6OHDA group; (C) images from rats in the IA group; and (D) images from rats in the 6OHDA+IA group. The black arrows indicate the dendritic order, namely the first, second, third and fourth dendrites. The white arrowheads indicate the dendritic spines of the striatal neurons. The right panel in (B) shows the dendritic spine loss in the striatal neurons of the 6OHDA group. 6OHDA, 6-hydroxydopamine; IA, ibotenic acid; Ctrl, control.

Decortication offsets dendrite lesions and spinal loss of striatal neurons in the PD rat model. Dendrites and dendritic spines are the main structures of striatal neurons. Therefore, Golgi staining was employed to investigate the morphological characteristics of the striatal neurons (27,31). LM analysis showed that the striatal neuronal dendrites were short, sparse and even broken in the 6OHDA group (Fig. 1). The statistical data showed that the total dendritic length of single neurons in the 6OHDA group (454.1±33.69 μm) was significantly decreased compared to that in the control group (615.6±42.44 μm; $P<0.05$; Fig. 2A), whereas the total dendritic length in the 6OHDA+IA group (586.4±50.72 μm) was significantly increased compared to that in the 6OHDA group ($P<0.05$; Fig. 2A).

The dendritic spines of the striatal neurons could be clearly observed in the brain slices using Golgi staining. Therefore, Golgi staining was also used to determine the dendritic spine density in the striatal neurons. The dendritic

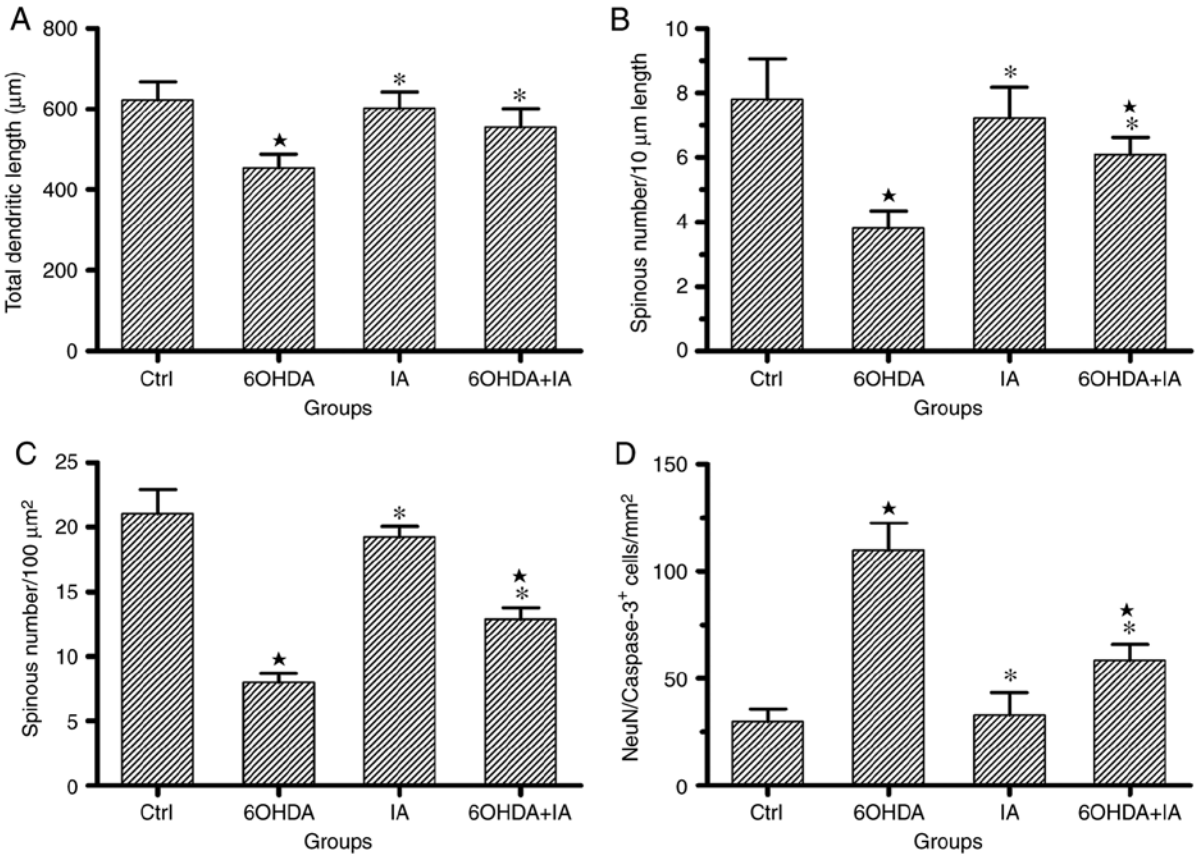

Figure 2. Statistical processing and comparisons of the experimental data. (A) Comparison of the total dendritic length of single neuron. An increased total dendritic length was observed in the 6OHDA + IA group compared with that in the 6OHDA group. (B) Comparison of the dendritic spine densities (spines/10 μm) as evaluated by Golgi staining, showing a severe loss of dendritic spines in the 6OHDA group. However, an increased density of dendritic spines was observed in the 6OHDA + IA rats compared to the density in the 6OHDA rats. (C) Comparison of the dendritic spine densities (number/100 μm^2) in the electron microscopy experiment, consistent with the Golgi staining experiment results. The statistical analysis showed a significant reduction in the dendritic spine density in the 6OHDA group, but an increase in the density in the 6OHDA + IA group. (D) Comparison of double-labeling immunofluorescence for NeuN/caspase-3, which shows a significant increase in the number of NeuN/caspase-3 double-labeled neurons in the 6OHDA group compared with the numbers in the control and 6OHDA + IA groups. Data are presented as the mean ± SD (n=6/group), two-way ANOVA. *P<0.05 vs. respective Ctrl group; *P<0.05 vs. respective 6OHDA group. NeuN, neuron-specific protein; Ctrl, control; 6OHDA, 6-hydroxydopamine; IA, ibotenic acid.

spine density was significantly downregulated in the 6OHDA group (3.8±0.53) compared with the density in the control group (7.80±1.26; P<0.05; Figs. 1 and 2B), whereas the dendritic spine density was upregulated in the 6OHDA+IA group (6.09±0.54) compared with the density in the 6OHDA group (P<0.05; Figs. 1 and 2B).

To investigate excitatory synaptic inputs on the dendritic spines, the microstructures of the striatal neurons were observed by EM. The dendritic spine density in the 6OHDA group (7.10±0.70) was significantly decreased compared to that in the control (21.07±1.83) and IA (19.24±0.82; P<0.05; Figs. 3 and 2C) groups. However, the dendritic spine density was significantly increased in the 6OHDA+IA group (12.89±0.8727) compared to that in the 6OHDA group (P<0.05; Figs. 3 and 2C). Similarly, no difference was observed between the control and IA (P>0.05; Figs. 3 and 2C) groups. These results suggested that decortication rescued the morphological alterations in the striatal neurons in the 6OHDA-treated rats.

Cortical regulation effects dopamine depletion-induced striatal neuron lesions. Apoptosis induced by dopamine deficiency contributes to the decrease in striatal neurons in PD. Thus, NeuN and caspase-3 expression was investigated in the experimental rat model. NeuN is a specific marker of neurons, whereas caspase-3 is a specific marker of apoptosis. Immunofluorescence analysis showed that the quantity of caspase-3-positive neurons was significantly upregulated in the 6OHDA group (110.00±12.62) compared to the quantity in the control group (29.79±6.06; P<0.05; Figs. 4 and 2D) and in the IA group (32.84±10.61; P<0.05; Figs. 4 and 2D). Notably, the quantity of caspase-3-positive neurons was downregulated in the 6OHDA + IA group (58.42±7.40) compared to the quantity in the 6OHDA group (P<0.05; Figs. 4 and 2D).

Western blotting and RT-qPCR analyses indicated that total caspase-3 expression was significantly upregulated in the 6OHDA group (1.80±0.20 and 0.28±0.03, respectively) compared to the control group (0.59±0.08 and 0.18±0.02, respectively; P<0.05; Fig. 5) and the IA group (0.73±0.03 and 0.24±0.04, respectively; P<0.05; Fig. 5). Similarly, total caspase-3 expression levels were decreased in the 6OHDA+IA group (0.75±0.07 and 0.20±0.02) compared to the expression levels in the 6OHDA group (P<0.05; Fig. 5). Western blotting indicated that cleaved caspase-3 expression was significantly upregulated in the 6OHDA group (1.430±0.19) compared to the control group (0.31±0.11; P<0.05; Fig. 5). Cleaved caspase-3 expression levels were decreased in the 6OHDA+IA

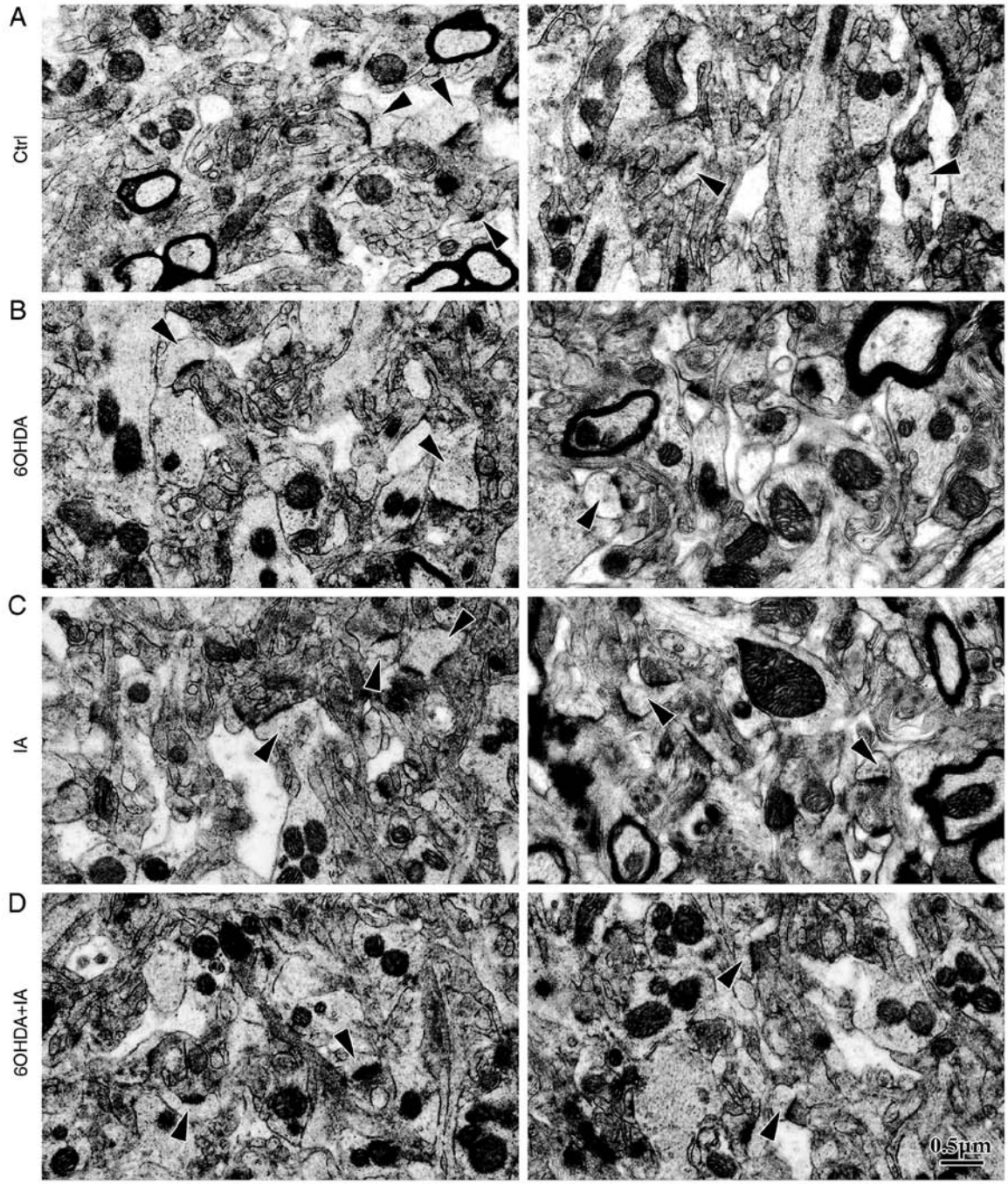

Figure 3. Detection of dendritic spines by electron microscopy. Dendritic spines of the striatal neurons from rats in (A) the control group, (B) the 6OHDA group, (C) the IA group and (D) the 6OHDA + IA group. The black arrowheads indicate the dendritic spines with excitatory synapse inputs. All images are at the same magnification. The left and right panels show two representative images for each group. 6OHDA, 6-hydroxydopamine; IA, ibotenic acid; Ctrl, control.

group (0.89±0.12) compared to the expression levels in the 6OHDA group ($P<0.05$; Fig. 5). These results demonstrated that decortication offset the downregulated apoptosis in the 6OHDA-treated rats.

In summary, these results suggested that decortication alleviated the abnormal morphology of striatal neurons and motor dysfunction in the 6OHDA-treated PD rat model.

Discussion

The results of the present study showed that partial decortication ameliorates the loss of dendritic spines on striatal neurons in the dopamine depletion-induced PD rat model. Researchers who study dendritic spines accept synaptic input frequency and the connection points provided by dendrites and spines as the basis of the structural integrity of the striatal synapses and the stability of the neural circuits, and their normal function is to maintain striatal function, while they are associated with neurodegenerative diseases (32). The striatum, which is a critical component of the basal ganglia, mainly consists of projection neurons and interneurons. In total, ~90% of all striatal neurons in rodents are striatal projection neurons. Interneurons make up ~10% of striatal neurons (33). The projection neurons comprise direct and indirect pathway

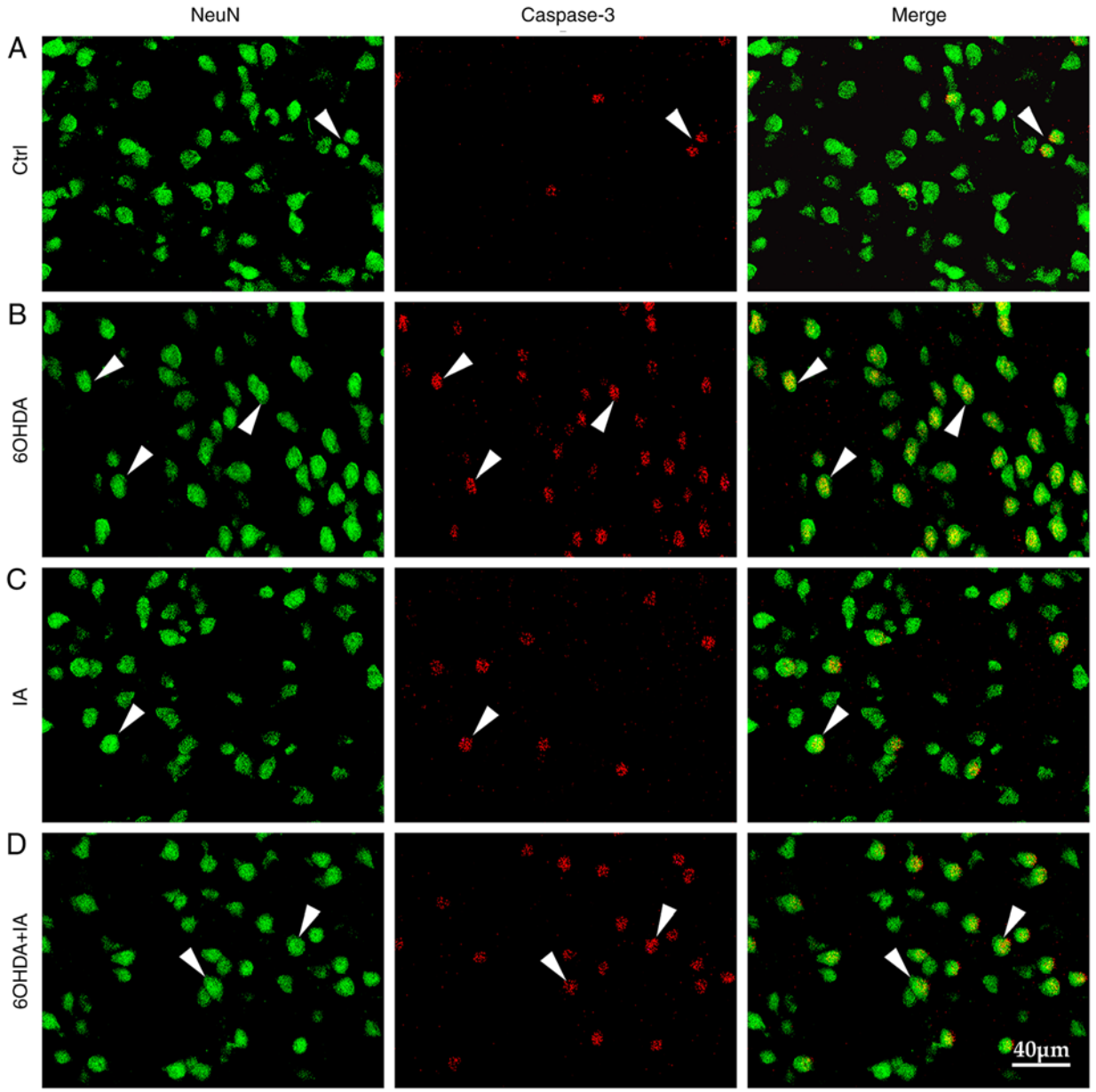

Figure 4. Detection of striatal neuronal apoptosis by double-label immunofluorescence. Striatal NeuN-positive cells (green), caspase-3-positive cells (red) and merged NeuN/caspase-3 in the striatum of rats in the (A) control, (B) 6OHDA, (C) IA and (D) 6OHDA + IA groups. The white arrows indicate representative caspase-3-positive neurons. 6OHDA, 6-hydroxydopamine; IA, ibotenic acid; Ctrl, control.

neurons. Direct and indirect pathway neurons have no significant distinctions in their morphology, quantity and distribution, and both secrete the inhibitory neurotransmitter γ-aminobutyric acid (GABA). However, the projection areas of the direct and indirect pathway neurons are different (34). The direct pathway neurons project to the substantia nigra pars reticulata (SNr), whereas indirect pathway neurons project to the SNr after relaying into the external segment of the globus pallidus and the subthalamic nucleus. As a crucial part of the motor center, the striatum plays an important role in muscular tension and fine motor behavior. The striatum also has a vital role in learning, memory and cognition (35-37). The function of the striatum relies on the projection neurons in the direct and indirect pathways. After transport to the SNr through the direct and indirect pathways and relaying in the thalamus, nerve impulses from striatal projection neurons regulate motor cortex activities. In addition, the activity of the striatal projection neurons is strictly regulated by interneurons and neurons from the cortex, thalamus and midbrain (38,39). Normally, the glutamatergic excitatory inputs from the cortex and thalamus and the dopaminergic inputs from the SNc coordinate with each other to maintain the functional stabilization and structural integrity of the striatal neurons (8).

It is generally known that the striatum is involved in various neurodegenerative diseases, such as PD and Huntington's disease (HD). Striatal neurons exhibit individual vulnerability in brain injury (39-41). For example, the projection neurons are vulnerable to ischemic damage, while the interneurons display resistance and even hyperplasia in middle cerebral artery occlusion models. The striatal projection neurons exhibit severe damage in HD, evidenced by the rupture of dendrites and dendritic spine loss (42). The funda-

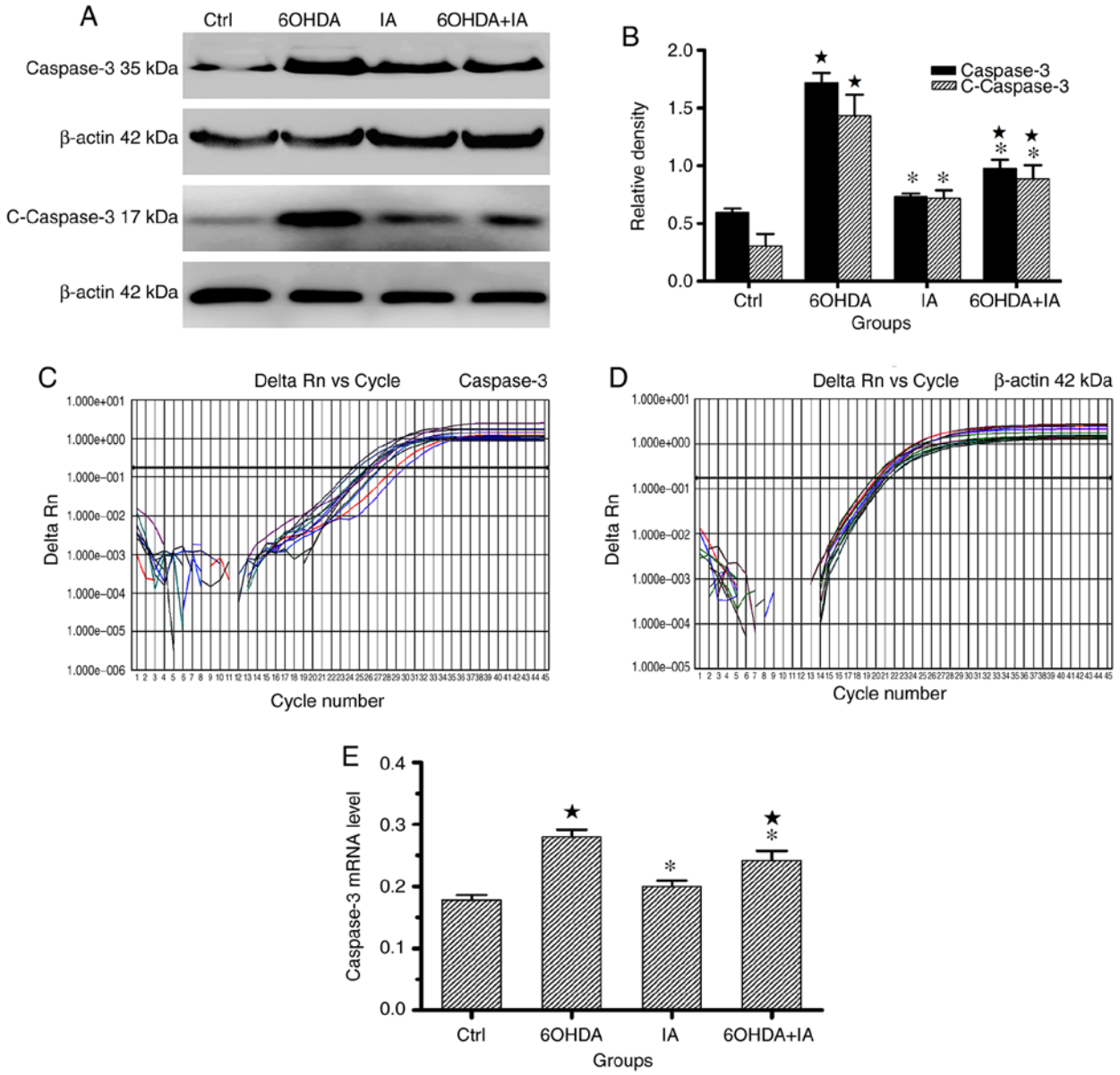

Figure 5. Detection and comparison of the striatal caspase-3 protein and mRNA levels. (A) Western blotting and (B) quantification showed that the total and cleaved caspase-3 protein level was significantly increased in the 6OHDA group compared with the level in the control group. The total and cleaved caspase-3 protein level was significantly decreased in the 6OHDA + IA group compared to the level in the 6OHDA group. The amplification curves of (C) caspase-3 mRNA and (D) β-actin mRNA are presented. (E) The total caspase-3 mRNA level in the 6OHDA group was significantly increased compared with those in the other three groups. The total caspase-3 mRNA level in the 6OHDA+IA group was significantly decreased compared to that in the 6OHDA group. Data are presented as the means ± SD (n=6/group), two-way ANOVA. *P<0.05 vs. respective Ctrl group; *P<0.05 vs. respective 6OHDA group. C-caspase-3, cleaved caspase-3; Ctrl, control; 6OHDA, 6-hydroxydopamine; IA, ibotenic acid.

mental cause of PD is the loss and dysfunction of dopaminergic neurons in the substantia nigra. Therefore, the question remains as to how dopamine deficiency in PD affects striatal neurons. Gerfen *et al* (38) found that the activity of striatal dopamine receptor D_2 neurons was upregulated in PD, with severe damage and loss of dendritic spines. However, striatal dopamine receptor D_1 neurons are not seriously affected. In the present study the quantity of caspase-3-positive neurons was increased in the 6OHDA-treated rats. In addition, western blotting and RT-qPCR further demonstrated that the expression of caspase-3 was upregulated at both the protein and mRNA levels. These results suggested that striatal neuron apoptosis did occur after dopamine was deleted. Dendritic spines that receive synaptic input are highly sensitive to injury. For example, striatal dendritic spines undergo severe loss in cerebral ischemia and HD (43,44). It was further demonstrated that the total dendritic length and dendritic density of the striatal projection neurons was decreased in the PD rats treated with 6OHDA.

Striatal projection neurons receive glutamatergic inputs from the cortex and thalamus, as well as dopaminergic inputs from the SNc. The balance of these synaptic inputs is critical to maintain the function and integrity of the striatum (45). The disruption of this balance between excitatory and inhibitory synaptic inputs (16), as well as that among DA, GABA and acetylcholine synaptic inputs (46), is the primary cause of striatal neuronal damage (47,48). To confirm this hypothesis, the present study evaluated the striatal dendritic regres-

sion in the PD rats treated with 6OHDA after decortication. Garcia *et al* (16) presented evidence of the glutamate depletion in the striatum following decortication. A noteworthy finding was that the decortication ameliorated neuronal dendritic lesions and dendritic spine loss. Moreover, the decortication also alleviated motor dysfunction in the PD rats. Other researchers have shown that dopamine depletion decreases grip strength (49); however previous studies (24,50), as well as the present study, reached the opposite conclusion (13). This inconsistency may be due to the different measurement methods and experimental animals. Other researchers have measured the grip strength of the forelimbs using a digital grip force meter; the animals are positioned to grab the grid with their forelimbs and are gently pulled to record the grip strength. The present study tested the duration and tension of grip strength, whereas other studies have tested the power of grip strength. On the other hand, the present results indicated that decortication alleviated the cognitive deficits induced by dopamine depletion. The striatal complexes in rodents can be roughly divided into the dorsolateral region (participating in sensorimotor circuits) and the ventromedial region (participating in associative circuits). Different striatal subregions receive inputs from distinct cortical areas and thus control different physiological functions, including the processes of learning and memory. The dorsolateral region analyzed by the present study receives inputs from the motor cortex (51). The striatum also receives input from other brain regions. A few areas of M1 were damaged. This may be the reason why there was no statistical difference between the IA group and the control group in the water maze test. However, the body weight of the animals was not assessed as part of the experiment and that is a limitation of the current work, and as such may guide future experiments. These results indicated that the presynaptic glutamatergic inputs offset the striatal neuronal lesions in 6OHDA-treated PD rats

In summary, the present study demonstrated that the relative excess of cortical excitatory inputs is important for striatal neuronal lesions in a PD rat model following treatment with 6OHDA, which shed new light on the pathology and treatment of PD.

Acknowledgements

The authors would like to thank Ms. Wanjun Guan (Core Lab Plat for Medical, Zhongshan School of Medicine, Sun Yat-sen University, China) for providing support for instruments and equipment, and Dr Ming Zhuang (The Frist Affiliated Hospital, Sun Yat-sen University) for providing advice on writing.

Funding

The present study was supported by the National Natural Science Foundation of China (grant no. 81471288) and by the National Key R&D Program of China (grant no. 2017YFA0104704).

Availability of data and materials

The datasets used and/or analyzed during the present study are available from the corresponding author on reasonable request.

Authors' contributions

WL and YZ designed the experiments. YZ, BL, XZ and JW performed all the experiments and drafted the manuscript. BL, XZ, JW and SC carried out data acquisition. SC, ZC, TC and ZH performed the data analysis. TC, ZH and WL participated in the revision of the manuscript. All authors read and approved the final manuscript.

Ethics approval and consent to participate

All rat care and procedures involved were approved by the Animal Care and Use Committee of Sun Yat-sen University (no. SYXK GUANGDONG 2011-0029).

Patient consent for publication

Not applicable.

Competing interests

The authors declare that they have no competing interests.

References

1. Hornykiewicz O: Dopamine (3-hydroxytyramine) and brain function. Pharmacol Rev 18: 925-964, 1966.
2. Gibb WR and Lees AJ: Anatomy, pigmentation, ventral and dorsal subpopulations of the substantia nigra, and differential cell death in parkinson's disease. J Neurol Neurosurg Psychiatry 54: 388-396, 1991.
3. Villalba RM and Smith Y: Differential striatal spine pathology in Parkinson's disease and cocaine addiction: A key role of dopamine. Neuroscience 251: 2-20, 2013.
4. Penney JB and Young AB: Speculations on the functional anatomy of basal ganglia disorders. Annu Rev Neurosci 6: 73-94, 1983.
5. DeLong MR: Primate models of movement disorders of basal ganglia origin. Trends Neurosci 13: 281-285, 1990.
6. Albin RL, Young AB and Penney JB: The functional anatomy of disorders of the basal ganglia. Trends Neurosci 18: 63-64, 1995.
7. DeLong MR and Wichmann T: Basal ganglia circuits as targets for neuromodulation in parkinson disease. JAMA Neurol 72: 1354-1360, 2015.
8. Kreitzer AC and Malenka RC: Striatal plasticity and basal ganglia circuit function. Neuron 60: 543-54, 2008.
9. Kreitzer AC: Physiology and pharmacology of striatal neurons. Annu Rev Neurosci 32: 127-147, 2009.
10. Parker JG, Marshall JD, Ahanonu B, Wu YW, Kim TH, Grewe BF, Zhang Y, Li JZ, Ding JB, Ehlers MD and Schnitzer MJ: Diametric neural ensemble dynamics in parkinsonian and dyskinetic states. Nature 557: 177-182, 2018.
11. Jimenez-Shahed J: A review of current and novel levodopa formulations for the treatment of parkinson's disease. Ther Deliv 7: 179-191, 2016.
12. Xiao D: Acupuncture for parkinson's disease: A review of clinical, animal, and functional magnetic resonance imaging studies. J Tradit Chin Med 35: 709-717, 2015.
13. Ma Y, Zhan M, OuYang L, Li Y, Chen S, Wu J, Chen J, Luo C and Lei W: The effects of unilateral 6-OHDA lesion in medial forebrain bundle on the motor, cognitive dysfunctions and vulnerability of different striatal interneuron types in rats. Behav Brain Res 1: 37-45, 2014.
14. Jia Y, Mo SJ, Feng QQ, Zhan ML, OuYang LS, Chen JC, Ma YX, Wu JJ and Lei WL: EPO-dependent activation of PI3K/Akt/FoxO3a signalling mediates neuroprotection in in vitro and in vivo models of parkinson's disease. J Mol Neurosci 53: 117-124, 2014.
15. Ma Y, Feng Q, Ouyang L, Mu S, Liu B, Li Y, Chen S and Lei W: Morphological diversity of GABAergic and cholinergic interneurons in the striatal dorsolateral and ventromedial regions of rats. Cell Mol Neurobiol 34: 351-359, 2014.

16. Garcia BG, Neely MD and Deutch AY: Cortical regulation of striatal medium spiny neuron dendritic remodeling in parkinsonism: Modulation of glutamate release reverses dopamine depletion-induced dendritic spine loss. Cereb Cortex 20: 2423-2432, 2010.
17. Mitchell IJ, Lawson S, Moser B, Laidlaw SM, Cooper AJ, Walkinshaw G and Waters CM: Glutamate-induced apoptosis results in a loss of striatal neurons in the parkinsonian rat. Neuroscience 63: 1-5, 1994.
18. Hernandez-Baltazar D, Mendoza-Garrido ME and Martinez-Fong D: Activation of GSK-3β and caspase-3 occurs in nigral dopamine neurons during the development of apoptosis activated by a striatal injection of 6-hydroxydopamine. PLoS One 8: e70951, 2013.
19. Shah M, Rajagopalan S, Xu L, Voshavar C, Shurubor Y, Beal F, Andersen JK and Dutta AK: The high-affinity D2/D3 agonist D512 protects PC12 cells from 6-OHDA-induced apoptotic cell death and rescues dopaminergic neurons in the MPTP mouse model of parkinson's disease. J Neurochem 131: 74-85, 2014.
20. General administration of quality supervision, inspection and quarantine of the People's Republic of China: Laboratory animal - Guideline for Ethical Review of Animal Welfare (GB/T 35892-2018). General Administration of Press and Publication of the People's Republic of China, Beijing, 2018. http://openstd.samr.gov.cn/bzgk/gb/newGbInfo?hcno=9BA619057D5C13103622A10FF4BA5D14
21. Deumens R, Blokland A and Prickaerts J: Modeling parkinson's disease in rats: An evaluation of 6-OHDA lesions of the nigrostriatal pathway. Exp Neurol 175: 303-317, 2002.
22. Zheng X, Wu J, Zhu Y, Chen S, Chen Z, Chen T, Huang Z, Wei J, Li Y and Lei W: A Comparative study for striatal-direct and-indirect pathway neurons to DA depletion-induced lesion in a PD rat model. Neurochem Int 118: 14-22, 2018.
23. Wu JJ, Chen S, Ouyang LS, Jia Y, Liu BB, Mu SH, Ma YX, Wang WP, Wei JY, Li YL, *et al*: Cortical regulation of striatal projection neurons and interneurons in a parkinson's disease rat model. Neural Regen Res 11: 1969-1975, 2016.
24. Shear DA, Dong J, Gundy CD, Haik-Creguer KL and Dunbar GL: Comparison of intrastriatal injections of quinolinic acid and 3-nitropropionic acid for use in animal models of Huntington's disease. Prog Neuropsychopharmacol Biol Psychiatry 22: 1217-1240, 1998.
25. Vorhees CV and Williams MT: Morris water maze: Procedures for assessing spatial and related forms of learning and memory. Nat Protoc 1: 848-858, 2006.
26. Mu S, Lin E, Liu B, Ma Y, OuYang L, Li Y, Chen S, Zhang J and Lei W: Melatonin reduces projection neuronal injury induced by 3-nitropropionic acid in the rat striatum. Neurodegener Dis 14: 139-150, 2014.
27. Garcia-Segura LM and Perez-Marquez J: A new mathematical function to evaluate neuronal morphology using the Sholl analysis. J Neurosci Methods 226: 103-109, 2014.
28. Graveland GA, Williams RS and DiFiglia M: A golgi study of the human neostriatum: Neurons and afferent fibers. J Comp Neurol 234: 317-333, 1985.
29. Deng YP, Wong T, Bricker-Anthony C, Deng B and Reiner A: Loss of corticostriatal and thalamostriatal synaptic terminals precedes striatal projection neuron pathology in heterozygous Q140 Huntington's disease mice. Neurobiol Dis 60: 89-107, 2013.
30. Livak KJ and Schmittgen TD: Analysis of relative gene expression data using real-time quantitative PCR and the 2(-Delta Delta C(T)) method. Methods 25: 402-408, 2001.
31. Wearne SL, Rodriguez A, Ehlenberger DB, Rocher AB, Henderson SC and Hof PR: New techniques for imaging, digitization and analysis of three-dimensional neural morphology on multiple scales. Neuroscience 136: 661-680, 2005.
32. Lammel S, Lim BK and Malenka RC: Reward and aversion in a heterogeneous midbrain dopamine system. Neuropharmacology 76 Pt B: 351-359, 2014.
33. Kawaguchi Y, Wilson CJ, Augood SJ and Emson PC: Striatal interneurones: Chemical, physiological and morphological characterization. Trends Neurosci 18: 527-535, 1995.
34. Gerfen CR and Surmeier DJ: Modulation of striatal projection systems by dopamine. Annu Rev Neurosci 34: 441-466, 2011.
35. Mowery TM, Penikis KB, Young SK, Ferrer CE, Kotak VC and Sanes DH: The sensory striatum is permanently impaired by transient developmental deprivation. Cell Rep 19: 2462-2468, 2017.
36. Zhai S, Tanimura A, Graves SM, Shen W and Surmeier DJ: Striatal synapses, circuits, and Parkinson's disease. Curr Opin Neurobiol 48: 9-16, 2018.
37. Radl D, Chiacchiaretta M, Lewis RG, Brami-Cherrier K, Arcuri L and Borrelli E: Differential regulation of striatal motor behavior and related cellular responses by dopamine D2L and D2S isoforms. Proc Natl Acad Sci USA 115: 198-203, 2018.
38. Gerfen CR: Indirect-pathway neurons lose their spines in parkinson disease. Nat Neurosci 9: 157-158, 2006.
39. Parker PR, Lalive AL and Kreitzer AC: Pathway-specific remodeling of thalamostriatal synapses in parkinsonian mice. Neuron 89: 734-740, 2016.
40. Yoshioka H, Niizuma K, Katsu M, Sakata H, Okami N and Chan PH: Consistent injury to medium spiny neurons and white matter in the mouse striatum after prolonged transient global cerebral ischemia. J Neurotrauma 28: 649-660, 2011.
41. de Oliveira PA, Ben J, Matheus FC, Schwarzbold ML, Moreira ELG, Rial D, Walz R and Prediger RD: Moderate traumatic brain injury increases the vulnerability to neurotoxicity induced by systemic administration of 6-hydroxydopamine in mice. Brain Res 1663: 78-86, 2017.
42. Beal MF, Ferrante RJ, Swartz KJ and Kowall NW: Chronic quinolinic acid lesions in rats closely resemble huntington's disease. J Neurosci 11: 1649-1659, 1991.
43. Graham RK, Pouladi MA, Joshi P, Lu G, Deng Y, Wu NP, Figueroa BE, Metzler M, André VM, Slow EJ, *et al*: Differential susceptibility to excitotoxic stress in YAC128 mouse models of huntington disease between initiation and progression of disease. J Neurosci 29: 2193-2204, 2009.
44. Chakraborty J, Nthenge-Ngumbau DN, Rajamma U and Mohanakumar KP: Melatonin protects against behavioural dysfunctions and dendritic spine damage in 3-nitropropionic acid-induced rat model of huntington's disease. Behav Brain Res 264: 91-104, 2014.
45. Sardi S, Vardi R, Sheinin A, Goldental A and Kanter I: New types of experiments reveal that a neuron functions as multiple independent threshold units. Sci Rep 7: 18036, 2017.
46. Shen W, Tian X, Day M, Ulrich S, Tkatch T, Nathanson NM and Surmeier DJ: Cholinergic modulation of Kir2 channels selectively elevates dendritic excitability in striatopallidal neurons. Nat Neurosci 10: 1458-1466, 2007.
47. Romashkova JA and Makarov SS: NF-kappaB is a target of AKT in anti-apoptotic PDGF signalling. Nature 401: 86-90, 1999.
48. Ruiz-Calvo A, Maroto IB, Bajo-Grañeras R, Chiarlone A, Gaudioso Á, Ferrero JJ, Resel E, Sánchez-Prieto J, Rodríguez-Navarro JA, Marsicano G, *et al*: Pathway-specific control of striatal neuron vulnerability by corticostriatal cannabinoid CB1 receptors. Cereb Cortex 28: 307-322, 2018.
49. Singh S and Kumar P: Neuroprotective potential of curcumin in combination with piperine against 6-hydroxy dopamine induced motor deficit and neurochemical alterations in rats. Inflammopharmacology 25: 69-79, 2017.
50. Leung TC, Lui CN, Chen LW, Yung WH, Chan YS and Yung KK: Ceftriaxone ameliorates motor deficits and protects dopaminergic neurons in 6-hydroxydopamine-lesioned rats. ACS Chem Neurosci 3: 22-30, 2012.
51. Packard MG and Knowlton BJ: Learning and memory functions of the basal ganglia. Annu Rev Neurosci 25: 563-593, 2002.